Prepared for submission to JHEP

arXiv:1404.0332v1 [hep-th] 1 Apr 2014

Open Verlinde line operators

Davide Gaiotto[1]

[1]*Perimeter Institute for Theoretical Physics*
31 Caroline Street North, ON N2L 2Y5, Canada

Abstract: We reformulate the action of Verlinde line operators on conformal blocks in a 3d TFT language and extend it to line operators labelled by open paths joining punctures on the Riemann surface. We discuss the possible applications of open Verlinde line operators to quantum Teichmüller theory, supersymmetric gauge theory and quantum groups

Contents

1 Introduction **1**

2 A 3d perspective **3**
2.1 Generalized conformal blocks 4
2.2 Verlinde line operators 7

3 Concrete calculations **9**

4 Examples **15**
4.1 Four-punctured sphere 18
4.2 One-punctured torus 20

5 Applications **22**
5.1 Open Verlinde line operators and quantum Teichmüller theory 22
5.2 Relation to q-deformed traffic rules and refined framed BPS degeneracies 25
5.3 Quantum groups 26

1 Introduction

Verlinde line operators are a class of linear operators which act on the space of conformal blocks for some current algebra [1], which in this note will always coincide with the Virasoro algebra. They are roughly labeled by a closed path ℓ on the Riemann surface, up to some subtleties which we will review momentarily. Traditionally, are defined by composing a sequence of elementary operations on conformal blocks, each corresponding to a map between spaces of conformal blocks which may differ in the number or type of insertions. Roughly speaking, one inserts an identity operator into the original conformal block, splits into two conjugate chiral operators ϕ_a and $\phi_{\bar{a}}$, transports ϕ_a along ℓ and then fuses the operators ϕ_a and $\phi_{\bar{a}}$ back to the identity channel.

Although originally defined in the context of 2d RCFTs, the definition works well for general Virasoro conformal blocks and give operators with interesting interpretations in the context of supersymmetric gauge theory [2–4].

This definition has some rough edges. The answer may depend on how the path ℓ winds around the auxiliary insertion $\phi_{\bar{a}}$ and it is not obvious that it will be independent

on the choice of starting point along ℓ. Typically, the normalization of the operator has to be set by hand. Experimentally, the Verlinde line operators satisfy nice skein relations, which again are not quite obvious from the definition and seem to imply a 3d TFT interpretation: the operators should really be labelled by paths drawn close to the Riemann surface into a three-dimensional geometry bounded by the surface itself.

An important observation is that Verlinde line operators are closely related to topological defects in CFTs. More precisely, if a CFT correlation function is represented as a pairing between anti-holomorphic and holomorphic conformal blocks, a Verlinde line operators inserted in the pairing should modify the correlation function precisely in the same way as a topological line defect with the same Cardy label as the original chiral operator ϕ_a [5]. This is at least true both in RCFTs and in almost-rational CFTs such as Liouville theory.

Topological line defects in RCFTs do have a neat 3d TFT interpretation [6] in terms of graphs embedded into a three-dimensional manifold, bound by two copies of the Riemann surface, where chiral and anti-chiral operators live. A secondary objective of this note will be to give a similar 3d TFT-inspired alternative definition of Verlinde line operators. The three-dimensional geometry will be a handle-body bounded by the Riemann surface, as appropriate for describing conformal blocks.

In the context of RCFTs, one can consider both topological defects wrapping closed paths and topological defects wrapping open paths ending at punctures. The main purpose of this note will be to extend the definition of Verlinde line operators to encompass operators labeled by open curves, which end at the punctures of the conformal block. Our definitions can be found in section 2.1 and concrete calculations in sections 3 and 4.

We will also describe briefly three applications of open Verlinde line operators, leaving a complete analysis to later publications. The first one is to establish a direct connection from the theory of BPZ conformal blocks to quantum Teichmüller theory: we will recover the quantum version of Fock coordinates as cross-ratios of open Verlinde line operators. This allows one to reverse the logic of standard constructions of quantum Teichmüller theory such as [7]. The second is to define the quantum deformation of the traffic rules used in computing framed BPS degeneracies for theories of the class A_1 [8]. The third is to clarify the relation between BPZ conformal blocks and quantum groups, and the identity between the fusion integral kernels and the quantum 6j symbols [9]. To do so, we will use a construction originally due to Witten in the context of Chern-Simons theory [10]. All applications are discussed in section 5.

2 A 3d perspective

A standard conformal block can be pictured as a trivalent graph Γ_0, representing a pair of pants decomposition of the Riemann surface. The graph should be thought of as embedded in the middle of the 3d handle-body associated to that decomposition, which fills in the Riemann surface by making the tubes of the pair of pants into solid cylinders. In genus zero, which will be our main source of examples, Γ_0 is a trivalent tree graph drawn inside a 3d ball, with external legs ending at the boundary of the ball.

Each edge of the graph is labeled by a representation of the Virasoro algebra, usually denoted by a choice of Liouville momentum. See Figure 1 for an example. In this note we will encounter both generic representations and degenerate representations of the Virasoro algebra. We will always impose the decoupling of null vectors for the degenerate representations, which implies specific selection rules on the Liouville momenta which flow through the graph.

We can denote a conformal block associated to the trivalent graph Γ_0 in a ket notation

$$|a_i\rangle_{\Gamma_0} \tag{2.1}$$

with a_i being the Liouville momenta on the edges. We will typically leave implicit the dependence on the complex structure parameters on the Riemann surface, and omit the Γ_0 subscript when unambiguous.

Conformal blocks associated to different pair of pants decompositions are related by linear transformations. Different pair of pants decompositions can be related by a sequence of elementary fusion and braiding moves (and the S transformation in positive genus), which are associated to well-known linear transformations. See Figure 2 for the pictorial representation of a fusion operation. A fusion operation which involves non-degenerate representations only is associated to an integral transformation with complicated integration kernel, as the s-channel conformal block is expressed as an integral over all possible t-channel Liouville momenta. If at least one of the representations involved is degenerate, then one deals with a much simpler, finite-dimensional linear transformation.

The standard definition of Verlinde line operators, and their open generalizations, involves a formal sequence of such fusion and braiding transformations. Our first step will be to introduce some 3d TFT-inspired definitions which help give a precise meaning to the intermediate steps of the calculation of Verlinde line operators.

For simplicity, we will restrict ourselves to situations where we encounter only the finite-dimensional fusion transformations associated to degenerate fields. Our abstract

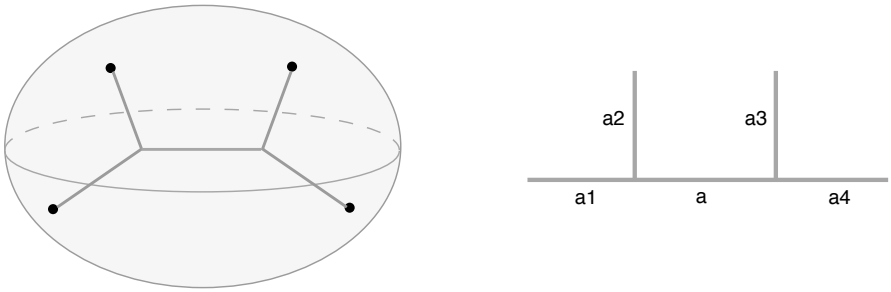


Figure 1. Left: the pictorial representation of a four-point conformal block, as a trivalent graph inside a ball. We omit for clarity the Liouville momentum labels on the edges. Right: The same conformal block, with the 3d ambient space omitted, and Liouville momenta labels on the edges.

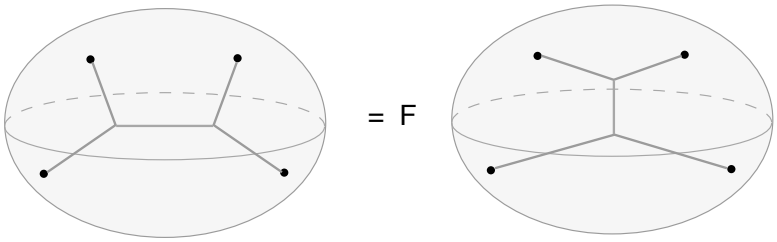


Figure 2. The pictorial representation of a fusion operation on the four-point conformal block. The fusion "matrix" F acts on the Liouville momentum label on the internal edge. It will be an integral kernel if the external edges carry a generic Liouville momentum, and a finite matrix if at least one external legs is degenerate

definitions could be generalized to the infinite-dimensional case in a straightforward way, but computations would be much harder.

2.1 Generalized conformal blocks

In order to do 3d TFT-like manipulations on conformal blocks, we will define a map from a much larger class of trivalent graphs in a fixed handle-body to the space of conformal blocks associated to a given pair of pants decomposition. The graphs may include many more loops and connected components than the basic trivalent graph Γ_0, but live in the handlebody associated to Γ_0.

The graphs must be refinements of the standard trivalent graph Γ_0 associated to the handle-body. More precisely, any such graph Γ must satisfy the following constraints:

- Each edge e_i^0 of Γ_0 will map to a consecutive sequence of edges $e_{i,u}$ in Γ.

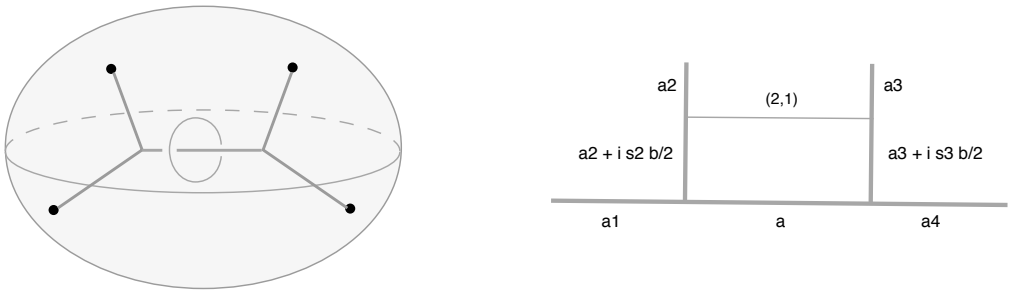


Figure 3. Left: a graph which refines the basic four-point graph Γ_0 in figure 1 by an extra degenerate loop linking the middle edge of Γ_0. We denote the degenerate loop by a thinner line. Right: a graph which refines the basic four-point graph Γ_0 by an extra rung. We omit the ambient three-ball and indicate the Liouville momenta. The $(2,1)$ label indicates the $\imath b + \imath b^{-1}/2$ degenerate momentum. The shifts s_2, s_3 take values ± 1

- The Liouville momenta on each collection of edges $e_{i,u}$ of Γ must differ by integral multiples of $\imath b/2$ and $\imath b^{-1}/2$ from the common value a_i associated to e_i^0 in Γ_0:

$$a_{i,u} = a_i + \imath s_{i,u} \frac{b}{2} + \imath \tilde{s}_{i,u} \frac{b^{-1}}{2} \tag{2.2}$$

- All other edges of Γ must carry degenerate representations. The graph Γ may include closed loops disconnected from the rest of the graph.

- At all vertices involving degenerate edges, the degenerate fusion rules must hold.

We will typically include the choice of degenerate representations in the new edges and of the s and $\tilde{s}$ shifts implicitly in the label "Γ". If we want to make the shifts explicit, we may refer to a graph $\Gamma[s, \tilde{s}]$. In concrete examples, our lines will be of type $(r, 1)$, and thus we will only need shifts s by multiples of $\imath b/2$, no $\tilde{s}$ shifts. Whenever we use the term "graph" from now on, we mean to denote such a decorated refinement of Γ_0.

We can describe two simple examples of graphs Γ, depicted in Figure 3:

- The union of Γ_0 and one or more closed loops linked to it

- A graph Γ obtained from Γ_0 by inserting an extra rung, a degenerate edge attached to two edges of Γ_0. Each end of the extra edge splits the corresponding edge of Γ_0 into two parts, with momenta which differ by an amount compatible with degenerate fusion.

The conformal block associated to a given graph Γ will be a finite linear combination of conformal blocks associated to Γ_0, with Liouville momenta shifted by appropriate multiples of b and b^{-1}:

$$|\Gamma; a_i\rangle_{\Gamma_0} = \sum_{n_i,\tilde{n}_i} c^{\Gamma_0;\Gamma}_{n_i,\tilde{n}_i} |a_i + n_i \frac{b}{2} + \tilde{n}_i \frac{b^{-1}}{2}\rangle_{\Gamma_0} \tag{2.3}$$

The sum will never include shifts of the Liouville momenta on external edges. By definition, $|\Gamma_0; a_i\rangle_{\Gamma_0} = |a_i\rangle_{\Gamma_0}$.

The coefficients $c^{\Gamma_0;\Gamma}_{n_i,\tilde{n}_i}$ will be rational functions in $\exp \pi b a_i$ and $\exp \pi b^{-1} a_i$ We can re-write the above relation in operatorial form, defining Weyl-commuting operators

$$\begin{aligned} \hat{\alpha}_i |a_i\rangle_{\Gamma_0} &= \exp \pi b a_i |a_i\rangle_{\Gamma_0} & \hat{\alpha}'_i |a_i\rangle_{\Gamma_0} &= \exp \pi b^{-1} a_i |a_i\rangle_{\Gamma_0} \\ \hat{p}_i |a_i\rangle_{\Gamma_0} &= |a_i + \imath b/2\rangle_{\Gamma_0} & \hat{p}'_i |a_i\rangle_{\Gamma_0} &= |a_i + \imath b^{-1}/2\rangle_{\Gamma_0} \end{aligned} \tag{2.4}$$

and thus

$$|\Gamma; a_i\rangle_{\Gamma_0} = \hat{O}_\Gamma |a_i\rangle_{\Gamma_0} \qquad \hat{O}_\Gamma = \sum_{n_i,\tilde{n}_i} c^{\Gamma_0;\Gamma}_{n_i,\tilde{n}_i}(\hat{\alpha}, \hat{\alpha}') \hat{p}_i^{n_i} (\hat{p}'_i)^{\tilde{n}_i} \tag{2.5}$$

We will drop the hats when possible to do so unambiguously to lighten the notation. Occasionally, we will also use the un-exponentiated operator

$$\hat{a}_i |a_i\rangle_{\Gamma_0} = a_i |a_i\rangle_{\Gamma_0} \tag{2.6}$$

The definition of these conformal blocks is recursive: if any pair of of graphs Γ and Γ' (which refine the same Γ_0) are related by a fusion or braiding move involving one of the extra degenerate edges, then the corresponding conformal blocks $|\Gamma; a_i\rangle_{\Gamma_0}$ and $|\Gamma'; a'_i\rangle_{\Gamma_0}$ are related by the corresponding linear relationship.

Furthermore, we are allowed to freely add or remove any number of rungs labeled by the identity representation, without changing the corresponding conformal blocks. If any subgraph is contained in a three-ball, whose boundary is crossed by a single edge which carries a representation different from the identity, the corresponding conformal block is zero. The final axiom is that a contractible loop labeled by a degenerate representation can be removed, multiplying the conformal block by the quantum dimension of the degenerate representation.

In order to compute $|\Gamma; a_i\rangle_{\Gamma_0}$, one simply applies a sequence of such moves to Γ, until it is reduced to Γ_0.

A good way to gain intuition on our construction is to depict conformal blocks as the result of a calculation in some 3d TFT, such as some kind of Chern-Simons theory [1], involving the handle-body geometry and a network Γ_0 of line defects. The space of

[1] It is unclear if such a 3d TFT truly exists for general conformal blocks. The closest to it is likely some construction involving a twisted $\mathcal{N} = 4$ SYM theory [11, 12].

conformal blocks is the Hilbert space associated to the boundary of the geometry, and the partition function with the network Γ_0 produces the specific basis element $|a\rangle$. Our $|\Gamma; a_i\rangle_{\Gamma_0}$ then should represent the answer to a 3d TFT calculation involving the same 3d geometry and the graph Γ of line defects. We set up the problem in such a way that Γ can be reduced to Γ_0 by using only 3d TFT manipulations involving degenerate lines.

2.2 Verlinde line operators

The action of a closed Verlinde line operators on a conformal block can be pictured as the insertion in the 3d manifold of an extra closed line, disconnected from the original graph, which runs just below the boundary along the path which labels the line operators. See Figure 4 for an example. The new line carries a specific degenerate Virasoro representation which also characterizes the choice of line defect. We can denote such a line, together with the choice of representation, with the symbol ℓ.

Given a graph Γ, which may or not coincide with the standard Γ_0, the addition of the extra line ℓ will produce a new graph $\ell \circ \Gamma$. The Verlinde line operator is a shift operator $\hat{O}_\ell$ defined as

$$\hat{O}_\ell \equiv \hat{O}_{\ell \circ \Gamma_0} \tag{2.7}$$

It is easy to see it satisfies the relation:

$$|\ell \circ \Gamma; a_i\rangle_{\Gamma_0} = \hat{O}_\ell |\Gamma; a_i\rangle_{\Gamma_0} \tag{2.8}$$

Indeed, we can do the sequence of manipulations which reduce Γ to Γ_0 first inside $\ell \circ \Gamma$, and then do the manipulations which reduce $\ell \circ \Gamma_0$ to Γ_0.

In particular,

$$|\ell_1 \circ \ell_2 \circ \Gamma; a_i\rangle_{\Gamma_0} = \hat{O}_{\ell_1} \hat{O}_{\ell_2} |\Gamma; a_i\rangle_{\Gamma_0} \tag{2.9}$$

etcetera. Operators labelled by lines which do not intersect when projected on the Riemann surface will commute, and the lines can be slipped through each other in the 3d geometry.

There is a simple strategy to compute $\hat{O}_\ell$. First one adds an extra line joining the new loop and the original graph, carrying a $(1, 1)$ (identity) representation. Then one applies fusion and braiding transformations until the graph is simplified back to Γ_0, together contractible loops which can be eliminated. See Figure 5 for the simplest example. It is easy to see that this definition essentially reproduces the original definition of the Verlinde line defect. Notice that $\hat{O}_\ell$ maps conformal blocks to conformal blocks with the same labels on external edges.

The definition of open line operators follows along similar lines. The action of an open line operators is represented by adding a rung a the trivalent graph Γ (without

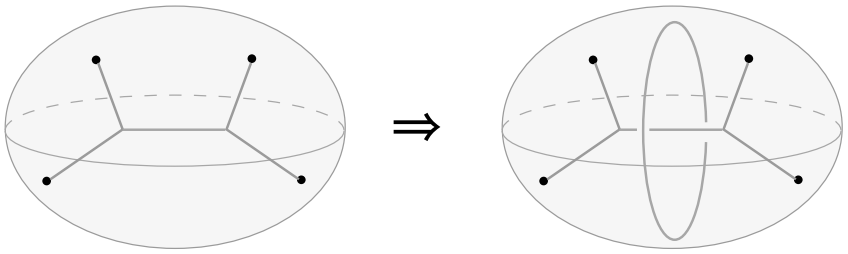


Figure 4. The pictorial representation of an "A-cycle" Verlinde line operator acting on a four-point conformal block. We omit for clarity the Liouville momentum labels on the edges

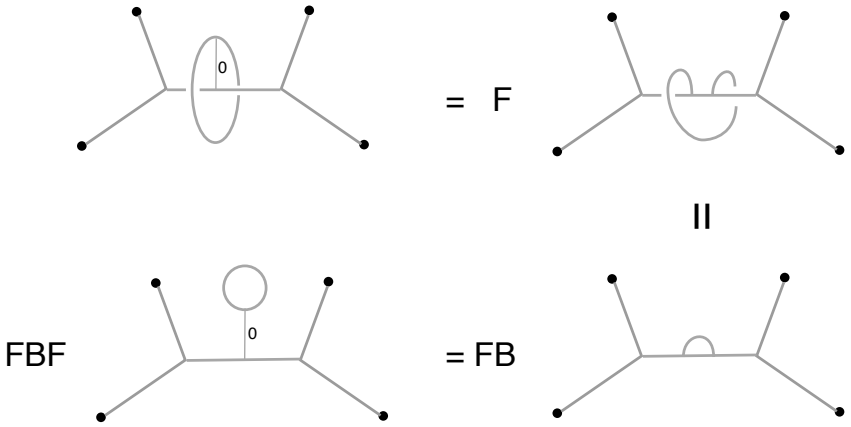


Figure 5. A graphical derivation of the sequence of fusion and braiding operations which realizes an A-cycle Verlinde line operator.

changing the geometry of the ambient 3-manifold!), which joins two external lines, say e_1 and e_2, and runs just below the boundary along the open path which labels the line operator. See Figure 6 for an example. The new rung splits each of the two external edges in two parts. On the part connected to the original Γ we keep the original external momenta of Γ. On the external part, we allow generic shifts s_1, s_2 and $\tilde{s}_1$, $\tilde{s}_2$ of the external momenta.

Thus the open line operator $\ell_{1,2}$ will be labelled by the choice of open path and the shifts of external momenta. If we denote the new decorated graph as $\ell_{1,2} \circ \Gamma$, we can thus define

$$\hat{O}_{\ell_{1,2}} \equiv \hat{O}_{\ell_{1,2} \circ \Gamma_0} \tag{2.10}$$

It is easy to see it satisfies the relation:

$$|\ell_{1,2} \circ \Gamma; a_i\rangle_{\Gamma_0} = \hat{O}_{\ell_{1,2}} |\Gamma; a_i\rangle_{\Gamma_0} \tag{2.11}$$

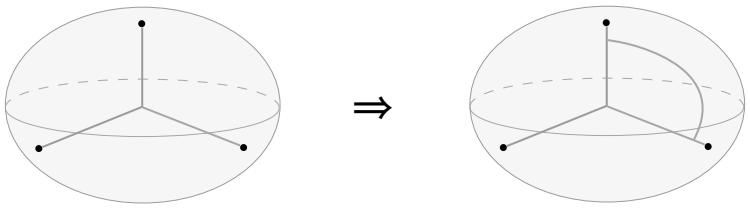


Figure 6. The pictorial representation of the action of an open Verlinde line operator on a three point conformal block. We omit for clarity the Liouville momentum labels on the edges

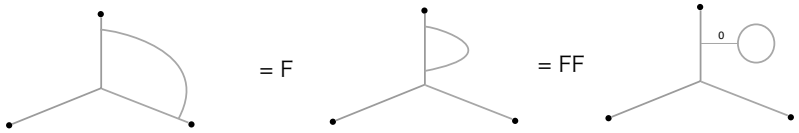


Figure 7. A graphical derivation of the sequence of fusion operations which realizes an open Verlinde line operator.

and that open and/or closed line operators compose nicely.

It is important to notice that the operator $\hat{O}_{\ell_{1,2}}$ include overall factors $p_1^{s_1}$, $p_2^{s_2}$, etc. which shift appropriately the external momenta. As traditional spaces of conformal blocks are usually defined for fixed external momenta, the open Verlinde operators maps distinct traditional spaces into each other. Operators labelled open lines which do not intersect when projected on the Riemann surface will commute.

3 Concrete calculations

A conformal block is built up from a pair of pants decomposition of the Riemann surface. The concrete construction of a generic conformal block involves several choices, such as a choice of local coordinate at each of the punctures of the three-punctured spheres one is gluing up together. Most local changes in these conventions are essentially immaterial, as they can be absorbed in a re-definition of the local coordinates on Teichmüller space. Global changes, though, do matter. A rotation of 2π in the local coordinate at an external puncture of conformal dimension Δ_a, for example, will rotate the conformal block by a phase $e^{2\pi i \Delta}$.

These facts can be expressed intrinsically as the statement that the conformal block is the section of some line bundle on Teichmüller space. Alternatively, one can pick some specific reference choices of local data, and keep track carefully of whenever these are changed. In either case, a useful way to keep track of the direction of the local

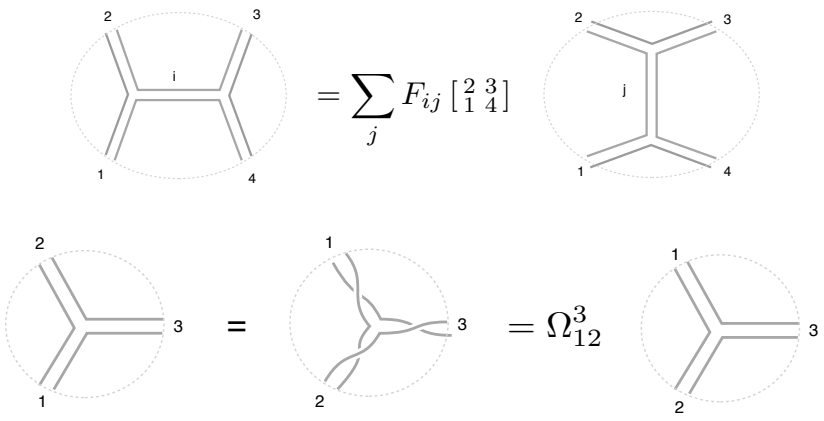


Figure 8. The A and B moves, in a ribbon graph representation

coordinate system at a puncture which is being transported around is to use ribbon graphs, which keep track of how many times the local coordinate rotates around the origin.

In genus zero, there is a simple choice of reference coordinate systems: keep the punctures near the equator of the sphere, and point the positive real axis of the local coordinate always in the same direction along the equator. Then all ribbons are flat in the plane of the picture, and we can draw them simply as lines without ambiguity. The basic manipulations of conformal blocs are A-moves, or fusion, which relates the two different ("s" and "t" channel) planar way to connect four lines, and B-moves, which exchange (braid) the position of two legs of a trinion. See Figure 8.

More precisely, the B-move is a combination of a half-twist of one leg (say with label i), and a half-twist of the other two legs of the trinion (say with labels j and k) in the opposite direction. This means that the two branches of the conformal block attached to j and k exchange place while the branch attached to i remains fixed, but neither of the three branches rotates. The conformal block is multiplied by a phase

$$\Omega^{i,\pm}_{jk} = e^{\pm \imath \pi(\Delta_i - \Delta_j - \Delta_k)} \tag{3.1}$$

It is also helpful to think about this in terms of an OPE: a conformal block with external punctures of dimensions Δ_j and Δ_k fused to a channel of dimension Δ_i will behave as $(z_j - z_k)^{\Delta_i - \Delta_j - \Delta_k}$. Thus the conformal block equals $\Omega^{i,+}_{jk}$ times a conformal block with k rotated clockwise around j. Notice that

$$\Omega^{i,+}_{jk} \Omega^{j,+}_{ik} = e^{-2\imath\pi\Delta_k} \tag{3.2}$$

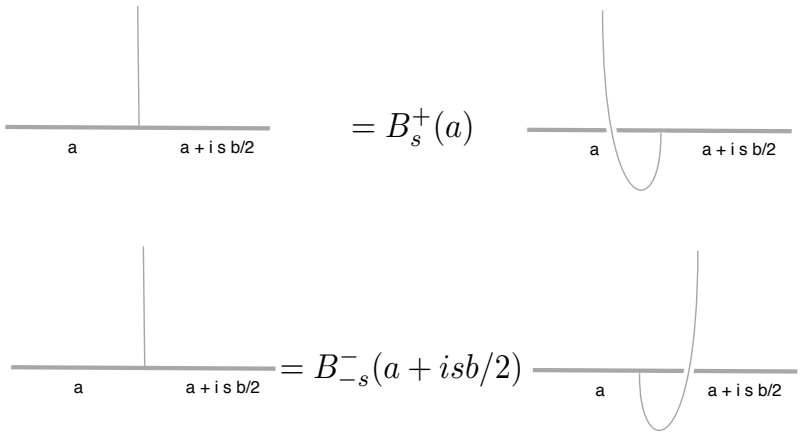


Figure 9. Two examples of a B move on a degenerate leg

In the following, we will denote generic Virasoro representations by a Liouville momentum $Q/2 + \imath a$, so that

$$\Delta_i = \frac{Q^2}{4} + a_i^2 \tag{3.3}$$

and $Q = b + b^{-1}$, while the central charge is $1 + 6Q^2$. We will also define

$$q = e^{\imath\pi b^2} \qquad\qquad \tilde{q} = e^{\imath\pi b^{-2}}. \tag{3.4}$$

Degenerate representations are labeled as (r, s), with Liouville momentum $a_{(r,s)} = \imath rb/2 + \imath sb^{-1}/2$, and corresponding dimension

$$\Delta_{r,s} = \left((1-r)b/2 + (1-s)b^{-1}/2\right)\left((1+r)b/2 + (1+s)b^{-1}/2\right). \tag{3.5}$$

The identity operator has label $(1, 1)$. Unless otherwise specified, we will focus on the degenerate field $(2, 1)$, indicated as a thin line in the figures. The basic building blocks we will use are the A and B moves involving a single $(2, 1)$ degenerate field.

If we specialize the k leg to be degenerate in $\Omega_{jk}^{i,\pm}$, and impose the degenerate fusion relation $a_j = a$, $a_i = a + isb/2$, $s = \pm 1$, we get

$$B_s^{\pm}(a) = \Omega_{j,(2,1)}^{i,\pm} = e^{\pm\imath\pi\left(\imath sba + b^2/2 + 1/2\right)} \equiv (-q)^{\pm\frac{1}{2}}\alpha^{\mp s} \tag{3.6}$$

Remember that $q = e^{\imath\pi b^2}$ and $\alpha = e^{\pi ba}$. It is useful to visualize this phase as being accrued when a degenerate insertion is moved from one side to the other of a non-degenerate leg of the graph, as in figure 9.

Next, consider a four-point conformal block on the sphere, with three generic legs of label a_1, a_2, a_3 and a single degenerate insertion. We want to consider the fusion

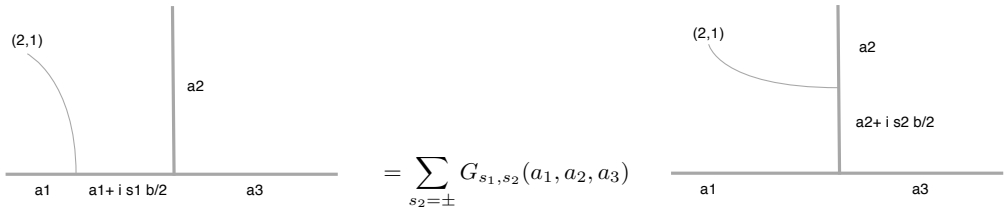


Figure 10. The A move on a degenerate leg

matrix

$$G_{s_1,s_2}(a_1,a_2,a_3) \equiv F_{a_1+\imath s_1 b/2, a_2+\imath s_2 b/2}\left[\begin{smallmatrix} a_{(2,1)} & a_2 \\ a_1 & a_3 \end{smallmatrix}\right] \tag{3.7}$$

which transports a degenerate insertion from the a_1 to the a_2 leg of a trivalent graph, as in figure 10. With an appropriate choice of normalization for the three point function, the matrix is

$$G_{s_1,s_2}(a_1,a_2,a_3) = \imath s_2 \frac{\cosh \pi b(a_3 + s_1 a_2 - s_2 a_1)}{\sinh 2\pi b a_2} = \imath s_2 \frac{\alpha_3 \alpha_2^{s_1} \alpha_1^{-s_2} + \alpha_3^{-1} \alpha_2^{-s_1} \alpha_1^{s_2}}{\alpha_2^2 - \alpha_2^{-2}} \tag{3.8}$$

$$\sum_{s_2=\pm 1} G_{s_1,s_2}(a_1,a_2,a_3) G_{s_2,s_1'}(a_2,a_1,a_3) = -s_1' \frac{\alpha_2^{-s_1-s_1'} - \alpha_2^{s_1+s_1'}}{\alpha_2^2 - \alpha_2^{-2}} = \delta_{s_1,s_1'} \tag{3.9}$$

A second check is an hexagon relation, where we alternate three A and three B moves in order to transport the degenerate field around a closed loop:

$$\sum_{s_2,s_3} G_{s1,s2}(a_1,a_2,a_3) B^{\pm}_{s_2}(a_2) G_{s2,s3}(a_2,a_3,a_1) B^{\pm}_{s_3}(a_3) G_{s3,s1'}(a_3,a_1,a_2) B^{\pm}_{s_3}(a_3)$$
$$= -e^{\pm \frac{3}{2} i\pi b^2} \delta_{s_1,s_1'}. \tag{3.10}$$

The phase factor originates from the fact that the local coordinate around the degenerate field is rotated by an angle of 2π in the process, as in figure 11.

We will need a few specializations of this formula as well. First, consider a situation where the third puncture is degenerate, $a_3 = \imath b + \imath b^{-1}/2$, and the other two satisfy the degenerate fusion so that $a_1 = a$ and $a_2 = a + \imath s_1 b/2 + \imath s b/2$. We are interested in the situation where $s = s_1$, i.e. where the two degenerate insertions shift the momentum a twice in the same direction. Then after the A move we must have $s_2 = -s_1$ as well, and the fusion matrix reduces to 1: two degenerate insertions which and on opposite sides of a line, and shift the momentum in the same direction commute. See figure 12.

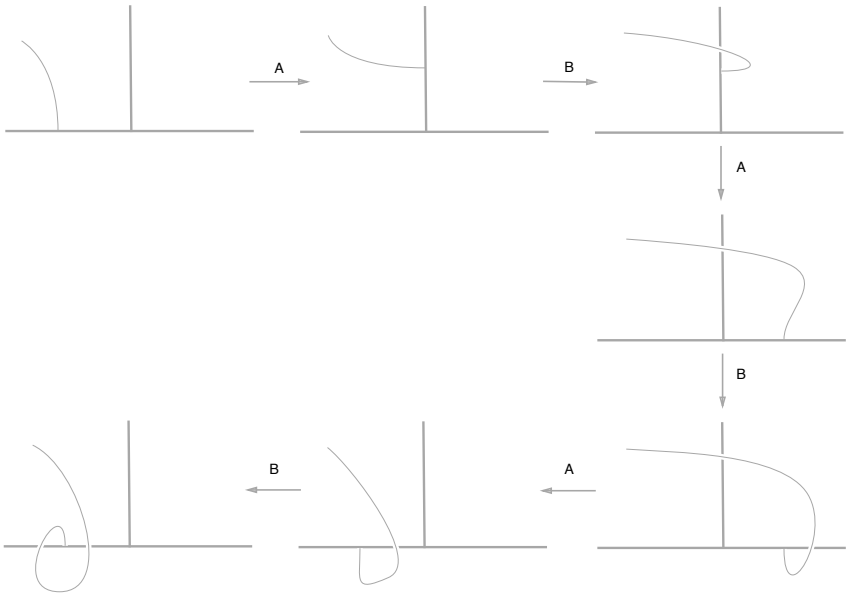


Figure 11. This sequence of A and B moves brings the conformal block back to itself up to a full twist of the degenerate leg

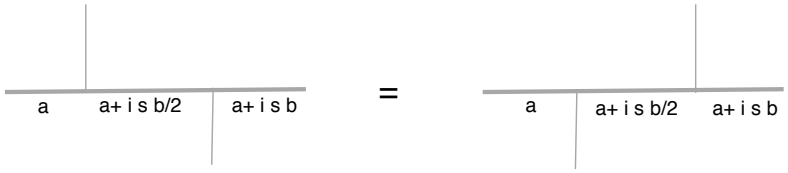


Figure 12. Two degenerate insertions on opposite sides commute if they shift the Liouville momentum in the same direction

Two degenerate insertions on the same side of an edge, which shift the Liouville momentum in the same direction, can be commuted across each other with the help of two braiding moves, to move one puncture on the opposite side of the edge and back. The result is that two such insertions Weyl commute, as in figure 13.

This can also be understood as follows: the two degenerate insertions can be fused by an A move, braided and unfused by another A-move. Although the OPE of two $(2,1)$ fields would usually contain both the identity and the $(3,1)$ field, the shift in the Liouville momenta imply that only the $(3,1)$ channel can contribute. The OPE in the $(3,1)$ channel behaves as $(z_1 - z_2)^{-\frac{b^2}{2}}$, and thus the braiding produces factors of $q^{\pm\frac{1}{2}}$.

If we take the second leg to be degenerate instead, we get the projection operator which can be used to fuse two nearby degenerate fields to the identity channel: we set

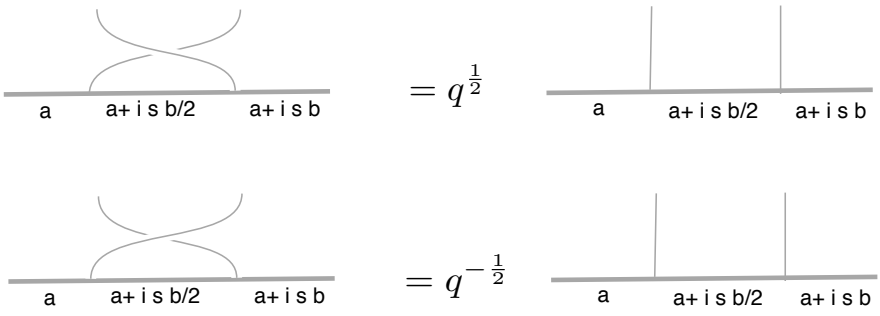


Figure 13. Two degenerate insertions on the same sides Weyl-commute if they shift the Liouville momentum in the same direction. The sign depends on the direction of the braiding

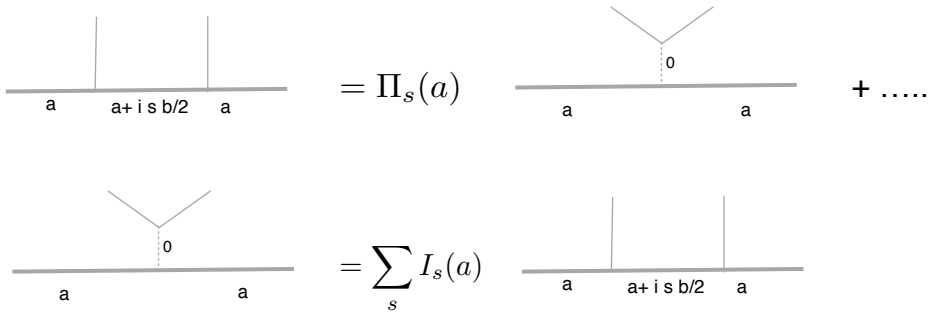


Figure 14. Fusion of degenerate fields to the identity and back. The ellipsis indicates an intermediate $(3,1)$ channel

$a_2 = \imath b + \imath b^{-1}/2$, $s_2 = -1$ and $a_3 = a_1 = a$, $s_1 = s$ to get

$$\Pi_s(a) = -s\frac{\sinh \pi b(2a + \imath sb)}{\sinh 2\pi \imath b^2} = -s\frac{\alpha^2 q^s - \alpha^{-2}q^{-s}}{q^2 - q^{-2}} \tag{3.11}$$

Viceversa, if we take the first leg to be degenerate, we get the map which splits an identity into two degenerate insertions: we set $a_1 = \imath b + \imath b^{-1}/2$, $s_1 = -1$, $a_3 = a_2 = a$ and $s_2 = s$ to get

$$I_s(a) = -s\frac{\sinh \imath \pi b^2}{\sinh 2\pi ba} = -s\frac{q - q^{-1}}{\alpha^2 - \alpha^{-2}} \tag{3.12}$$

See figure 14

It is also useful to derive the skein relation for degenerate lines. We can start from the second relation in figure 14, specialized to $a = a_{(2,1)} = \imath b + \imath b^{-1}/2$, so that we expand the identity t-channel conformal block f_t in s-channel blocks.

The coefficient $I_{-1}(a_{(2,1)})$ of the identity s-channel conformal block f_s is $-(q + q^{-1})^{-1}$. We can braid the two degenerate legs on the left to get the expansion of an

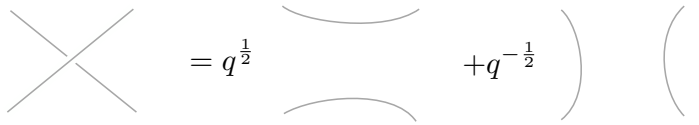


Figure 15. Skein relation for $(2,1)$ degenerate edges



Figure 16. A closed contractible loop evaluates to a quantum dimension which is determined from the skein relation applied to a figure eight

identity u-channel block $f_u^{\pm}$, and take a linear combination of the two formulae to project away the $(3,1)$ s-channel block. The result is

$$f_u^{\pm} - q^{\pm 1/2} f_t = (q+q^{-1})^{-1} q^{\mp 3/2} \left(1+q^{\pm 2}\right) f_s = q^{\mp 1/2} f_s \tag{3.13}$$

which is the expected skein relation, depicted in figure 15. If we apply the skein relation to a figure eight closed loop, as in figure 16, we get a constraint on the quantum dimension $d_{(2,1)}$: a contractible loop evaluates to

$$d_{(2,1)} = -q - q^{-1} \tag{3.14}$$

This is all the information we need to compute open and closed Verlinde line operators.

4 Examples

It is useful to start from a somewhat trivial example of decorated graph Γ: a single extra degenerate line which starts and ends on the same edge of a graph Γ_0, as in figure 17. We may simply fuse the two insertions to produce a tadpole graph, which by our axioms projects the intermediate channel to the identity. We can thus remove the identity line, and contract away the closed degenerate loop to remove the degenerate line. The final result is a conformal block without decorations, multiplied by the "bubble factor"

$$A_s[a]|a\rangle_{\Gamma_0} = -(q+q^{-1})\Pi_s(a)|a\rangle_{\Gamma_0} = \frac{\alpha^{2s}q - \alpha^{-2s}q^{-1}}{q-q^{-1}}|a\rangle_{\Gamma_0} \tag{4.1}$$

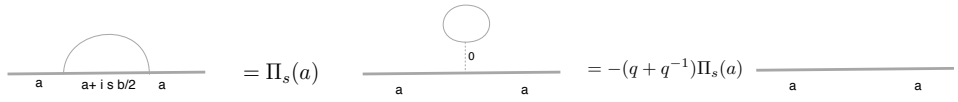


Figure 17. An almost trivial "bubble" decoration

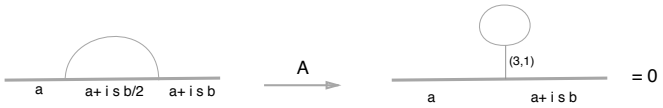


Figure 18. An "bubble" decoration which vanishes due to our axioms

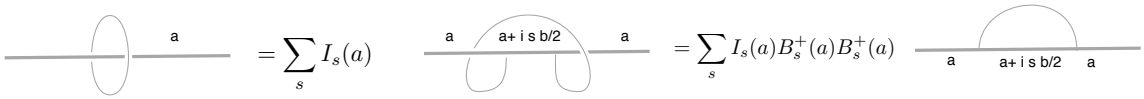


Figure 19. The reduction of a basic closed Verlined line defect to a bubble decoration

Notice that a similar bubble diagram with different Liouville momenta in the external legs, as in figure 18, will always vanish because of our axioms: the degenerate fusion requires the intermediate channel attached to the closed loop differ from the identity, and it is thus projected to zero.

The most basic example of closed Verlinde line operator is associated to an A-type loop, a closed degenerate loop winding an edge of the graph Γ_0, as in figure 19. It can be evaluated to

$$\sum_s \Pi_s(a) B_s^+(a) B_s^+(a) A_s[a] |a\rangle_{\Gamma_0} = \left(\alpha^2 + \alpha^{-2}\right) |a\rangle_{\Gamma_0} \tag{4.2}$$

It is also possible to compute the multiplicative coefficient for a multiple-wound loop:

$$\sum_s \Pi_s(a) \left[B_s^+(a)\right]^{2n} \frac{\alpha^{2s} q - \alpha^{-2s} q^{-1}}{q - q^{-1}} = q^{n-1} \frac{\alpha^{2n+2} - \alpha^{-2n-2}}{\alpha^2 - \alpha^{-2}} - q^{n+1} \frac{\alpha^{2n-2} - \alpha^{-2n+2}}{\alpha^2 - \alpha^{-2}} \tag{4.3}$$

Next, we can look at examples involving a single trinion in Γ_0. It can be computed from a triangle diagram T_{s_1,s_2} with a degenerate line connecting consecutive edges of a trinion T_0, as in figure 20. If we write

$$|T_{s_1,s_2}; a_1, a_2, a_3\rangle = T_{s_1,s_2}[a_1, a_2, a_3] |a_1, a_2, a_3\rangle \tag{4.4}$$

then we can compute

$$T_{s_1,s_2}[a_1, a_2, a_3] = -1 \frac{\alpha_3 \alpha_2^{s_1} \alpha_1^{s_2} q^{\frac{s_1 s_2}{2}} + \alpha_3^{-1} \alpha_2^{-s_1} \alpha_1^{-s_2} q^{\frac{-s_1 s_2}{2}}}{q - q^{-1}} \tag{4.5}$$

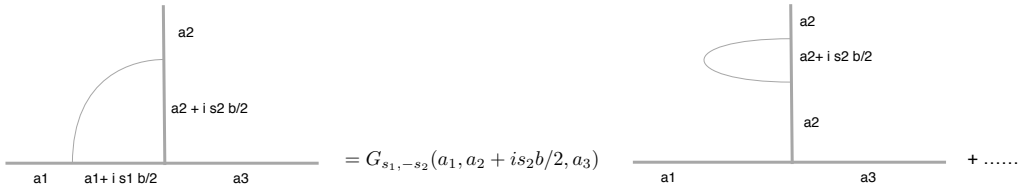


Figure 20. The computation of the triangle diagram T_{s_1,s_2} used in the definition of the open Verlinde line defect $\mathcal{O}_{1,2}^{-s_1,-s_2}$. The ellipsis indicates a term with Liouville momentum $a_2 + \imath s_2 b$ in the fusion channel, which vanishes as in figure 18

We can do some checks of this expression, and our formalism, by specializing some of the external legs to degenerate values and imposing degenerate fusion. For example, if we take the second leg to be degenerate of type $(1,1)$, i.e. the identity, so that we have $\alpha_2 = \imath q^{1/2}$, $s_2 = 1$, $s_1 = s$ and $a_1 = a_3 = a$, the triangle reduces to the the bubble factor. If we take the second leg to be degenerate of type $(2,1)$, $\alpha_2 = \imath q$, $s_2 = -1$, $\alpha_3 = q^{s_1/2}\alpha_1$, so that the intermediate momentum on the second leg is that of the identity, we get 1.

If we take the second leg to be degenerate of type $(3,1)$, $\alpha_2 = \imath q^{3/2}$, $s_2 = -1$, $\alpha_3 = q^{s_1/2+s_1'/2}\alpha_1$, so that the intermediate momentum on the second leg is of type $(2,1)$, we get a $(3,1)$ external leg which splits into two $(2,1)$ legs and the corresponding factor is $q+q^{-1}$ if $s_1 = s_2$, 1 otherwise. We can call the latter special triangle coefficient "splitting factor" $S_{s_1,s_1'}[a_1]$. This is a very useful piece of information to study graphs which include a $(3,1)$ leg.

For example, consider a trinion with two consecutive $(2,1)$ rungs inserted on it, of shifts s_1, s_2 and s_1', s_2' respectively. We can reduce it to the basic undecorated trinion multiplied by

$$T_{s_1,s_2}[a_1, a_2, a_3] T_{s_1',s_2'}[a_1 + \imath s_1 b/2, a_2 + \imath s_2 b/2, a_3]. \tag{4.6}$$

On the other hand, we can add a trivial $(1,1)$ rung between the two parallel $(2,1)$ lines and fuse it into a $(3,1)$ line or an $(1,1)$ line. The former can be simplified to a simple triangle diagram with a $(3,1)$ rung with the help of the splitting factors. The latter can be simplified with two bubble factors. We expect thus a relation

$$\begin{aligned} T_{s_1,s_2}[a_1, a_2, a_3] T_{s_1',s_2'}[a_1 + \imath s_1 b/2, a_2 + \imath s_2 b/2, a_3] = \\ = I_1(a_{(2,1)}) S_{s_1,s_1'}[a_1] S_{s_2,s_2'}[a_2] T^{(3,1)}_{s_1+s_1',s_2+s_2'}[a_1, a_2, a_3] + \\ + I_0(a_{(2,1)}) \delta_{s_1+s_2',0} \delta_{s_2+s_2',0} A_{s_1}(a_1) A_{s_2}(a_2) \end{aligned} \tag{4.7}$$

It is easy to check that these 16 relations are compatible with each other, and define uniquely the 9 operators $T^{(3,1)}_{s_1,s_2}[a_1, a_2, a_3]$. This procedure can be iterated to

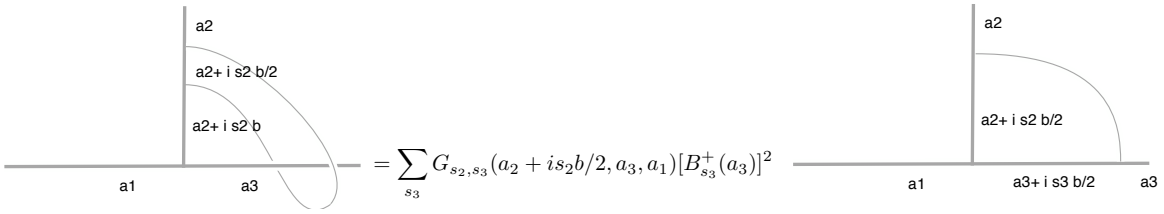


Figure 21. The computation of the decorated trinion L_{s_2} used in the definition of an open Verlinde line defect with both ends on the same external leg.

derive systematically triangles $T^{(k,1)}_{s_1,s_2}[a_1, a_2, a_3]$ with the extra rungs labelled by higher degenerate representations.

We are ready to write down the open Verlinde line operator $\mathcal{O}^{s_1,s_2}_{1,2}$ acting on the 1 and 2 legs of the trinion.

$$\begin{aligned}\mathcal{O}^{s_1,s_2}_{1,2}|a_1, a_2, a_3\rangle &= |T_{-s_1,-s_2}; a_1 + \imath s_1 b/2, a_2 + \imath s_2 b/2, a_3\rangle = \\ &= -\imath \frac{\hat{\alpha}_3 \hat{\alpha}_2^{-s_1} \hat{\alpha}_1^{-s_2} q^{\frac{s_1 s_2}{2}} + \hat{\alpha}_3^{-1} \hat{\alpha}_2^{s_1} \hat{\alpha}_1^{s_2} q^{\frac{-s_1 s_2}{2}}}{q - q^{-1}} \hat{p}_1^{s_1} \hat{p}_2^{s_2} |a_1, a_2, a_3\rangle \end{aligned} \tag{4.8}$$

An important and non-trivial check is the observation that the operators $\mathcal{O}^{s_1,s_2}_{1,2}$, $\mathcal{O}^{s_2,s_3}_{2,3}$ and $\mathcal{O}^{s_3,s_1}_{3,1}$ for given s_i acting on a three-punctured sphere commute, as they should, as they end on opposite sides of the same line, and shift the Liouville momentum in the same direction. For each choice of three s_i we can find an alternative normalization of the three-point conformal block such that the $\mathcal{O}^{s_i,s_j}_{i,j}$ reduce to $p_i^{s_i} p_j^{s_j}$.

Later, we will also need to consider an open Verlinde line operator we can associate to a trinion, which starts and ends on the same leg, and shifts the corresponding momentum twice in the same direction, is based on figure 21. We can compute the appropriate coefficient here:

$$\begin{aligned} L_{s_2}[a_1, a_2, a_3] = \sum_{s_3} s_3 &\frac{\alpha_1 \alpha_3^{s_2} \alpha_2^{-s_3} q^{-1/2} + \alpha_1^{-1} \alpha_3^{-s_2} \alpha_2^{s_3} q^{1/2}}{\alpha_3^2 - \alpha_3^{-2}} \cdot \\ &(-q) \alpha_3^{-2 s_3} \frac{\alpha_1 \alpha_3^{s_2} \alpha_2^{s_3} q^{\frac{s_2 s_3}{2}} + \alpha_1^{-1} \alpha_3^{-s_2} \alpha_2^{-s_3} q^{\frac{-s_2 s_3}{2}}}{q - q^{-1}} \end{aligned} \tag{4.9}$$

4.1 Four-punctured sphere

Next, we can consider the action of open Verlinde line operators on a four-point sphere s-channel conformal block, as in the top left corner of Figure 8. The open Verlinde line operators joining directly the 1 and 2 edges, or the 3 and 4 edges, $O^{s_1,s_2}_{1,2}$ and $O^{s_3,s_4}_{3,4}$, are

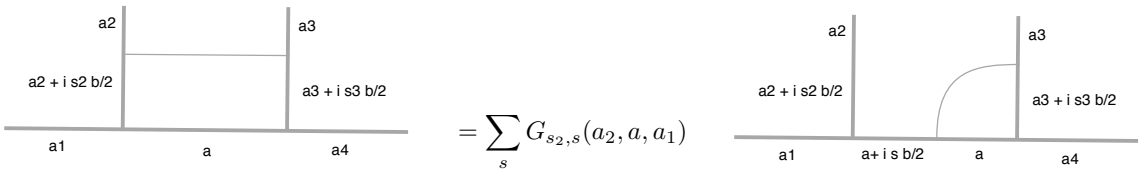


Figure 22. The computation of the coefficients for a rectangular graph conformal block $R^s_{s_2,s_3}[a_1, a_2, a_3, a_4, a]$

obviously the same as we found for the trinion:

$$\begin{aligned}\mathcal{O}^{s_1,s_2}_{1,2}|a_i; a\rangle &= -\imath\frac{\hat\alpha\hat\alpha_2^{-s_1}\hat\alpha_1^{-s_2}q^{\frac{s_1s_2}{2}} + \hat\alpha^{-1}\hat\alpha_2^{s_1}\hat\alpha_1^{s_2}q^{\frac{-s_1s_2}{2}}}{q-q^{-1}}\hat p_1^{s_1}\hat p_2^{s_2}|a_i; a\rangle \\ \mathcal{O}^{s_3,s_4}_{3,4}|a_i; a\rangle &= -\imath\frac{\hat\alpha\hat\alpha_4^{-s_3}\hat\alpha_3^{-s_4}q^{\frac{s_3s_4}{2}} + \hat\alpha^{-1}\hat\alpha_4^{s_3}\hat\alpha_3^{s_4}q^{\frac{-s_3s_4}{2}}}{q-q^{-1}}\hat p_3^{s_3}\hat p_4^{s_4}|a_i; a\rangle \end{aligned} \tag{4.10}$$

There are two natural operators which join directly the punctures 2 and 3 and 1 and 4, which we can denote as $O^{s_2,s_3}_{2,3}$ and $O^{s_4,s_1}_{4,1}$. The operator $O^{s_2,s_3}_{2,3}$ is computed from the coefficients for a rectangular graph in figure 22 as

$$O^{s_2,s_3}_{2,3}|a_i, a\rangle = \sum_{s=\pm1}\hat p^s R^s_{-s_2,-s_3}[\hat a_1, \hat a_2, \hat a_3, \hat a_4, \hat a]\hat p_2^{s_2}\hat p_3^{s_3}|a_i; a\rangle \tag{4.11}$$

where

$$\begin{aligned}R^s_{s_2,s_3}[a_1, a_2, a_3, a_4, a] &= G_{s_2,s}(a_2, a, a_1)T_{-s,s_3}[a + \imath sb/2, a_3, a_4] \\ &= s\frac{\alpha_1\alpha^{s_2}\alpha_2^{-s} + \alpha_1^{-1}\alpha^{-s_2}\alpha_2^s}{\alpha^2-\alpha^{-2}}\frac{\alpha_4\alpha_3^{-s}\alpha^{s_3} + \alpha_4^{-1}\alpha_3^s\alpha^{-s_3}}{q-q^{-1}}\end{aligned} \tag{4.12}$$

Notice the position of the $\hat p$ operators in the expression for $O^{s_2,s_3}_{2,3}$, and remember that

$$\hat p\hat a = (\hat a - \imath b/2)\hat p \qquad\qquad \hat p_i\hat a_i = (\hat a_i - \imath b/2)\hat p \tag{4.13}$$

Similarly,

$$O^{s_4,s_1}_{4,1}|a_i, a\rangle = \sum_{s=\pm1}\hat p^s R^s_{-s_4,-s_1}[\hat a_1, \hat a_2, \hat a_3, \hat a_4, \hat a]\hat p_4^{s_4}\hat p_1^{s_1}|a_i; a\rangle \tag{4.14}$$

By commuting with a B-move $\Omega^{a,\pm}_{12}$ we can easily derive simple operators $O^{s_1,s_3,\pm}_{1,3}$ and $O^{s_2,s_4,\pm}_{2,4}$ which join the corresponding punctures passing above or below the graph.

With sufficient patience, one can verify the expected Weyl commutation relations between operators with the same set of s_i. A less trivial, but ultimately straightforward,

task is to verify that these operators are compatible with the fusion and braiding transformations on Γ_0. In other words, the know fusion integral kernel $F_{a,a'}[a_i]$ which maps s-channel and t-channel bases of conformal blocks into each other as in figure 2 intertwines the corresponding expressions for the $O_{ij}^{s_i,s_j}$ operators acting on the two bases of conformal blocks. Conversely, such intertwining formulae can be interpreted as difference equations satisfied by the fusion and braiding kernels. It would be interesting to pursue this line of inquiry further, possibly for other current algebras.

We can do a few useful checks of the correctness of the expression for the $R^s_{s_2,s_3}$ coefficient. For example, if we set a_2 to the value for the identity, and $s_2 = 1$, $a = a_1 \pm \imath b/2$, we can recover the appropriate triangle $T_{\pm,s_3}(a_1, a_3, a_4)$. Also, we can compute the rectangle coefficient R in an alternative way: fuse the two parallel horizontal rung and then compute the resulting triangles:

$$R^s_{s_2,s_3}[a_1, a_2, a_3, a_4, a] = I_s(a) T_{s_2,-s}[a_2, a + \imath s b/2, a_1] T_{-s,s_3}[a + \imath s b/2, a_3, a_4] \tag{4.15}$$

We can consider a double-rectangle, with $(2, 1)$ rungs between the second and third legs of Γ_0 and compute it by first reducing the top rectangle and then the bottom, or viceversa. Concretely, that gives the identity

$$\begin{aligned} &\sum_{s|s'-s=\pm 1} R^s_{s_2,s_3}[a_1 + \imath s_1 b/2, a_2, a_3, a_4 + i s_4 b/2, a] R^{s'-s}_{s_4,s_1}[a_3, a_4, a_1, a_2, a + \imath s b/2] = \\ = &\sum_{s|s'-s=\pm 1} R^{s'-s}_{s_2,s_3}[a_1, a_2, a_3, a_4, a + \imath s b/2] R^s_{s_4,s_1}[a_3 + \imath s_3 b/2, a_4, a_1, a_2 + \imath s_2 b/2, a] \end{aligned} \tag{4.16}$$

where s' can be 2,0,or -2. This is useful in checking that $O^{s_2,s_3}_{2,3}$ and $O^{s_4,s_1}_{4,1}$ commute.

We can also use the rectangle coefficient specialized to degenerate values of a to fuse parallel rungs in some generic graph. We will do so in a later section. Here we report the relevant coefficients: if we specialize a to a $(k+1, 1)$ degenerate momentum, $a_1 = a_2 + \imath(s_2 + s'_2)b/2$, $a_4 = a_3 + \imath(s_3 + s'_3)b/2$, we get the coefficients

$$\begin{aligned} C^{k;s}_{s_2,s_3;s'_2,s'_3}[a_2, a_3] = s s_2 s_3 &\frac{\alpha_2^{1-s} q^{s_2(k+2)/2 + s'_2/2} - \alpha_2^{s-1} q^{-s_2(k+2)/2 - s'_2/2}}{q^{k+1} - q^{-k-1}} \cdot \\ \cdot &\frac{\alpha_3^{1-s} q^{s_3(k+2)/2 + s'_3/2} - \alpha_3^{s-1} q^{-s_3(k+2)/2 - s'_3/2}}{q - q^{-1}} \end{aligned} \tag{4.17}$$

4.2 One-punctured torus

The next classical example of closed Verlinde line operator wraps a B-cycle of the one-punctured torus. We will denote as a the Liouville momentum running in the

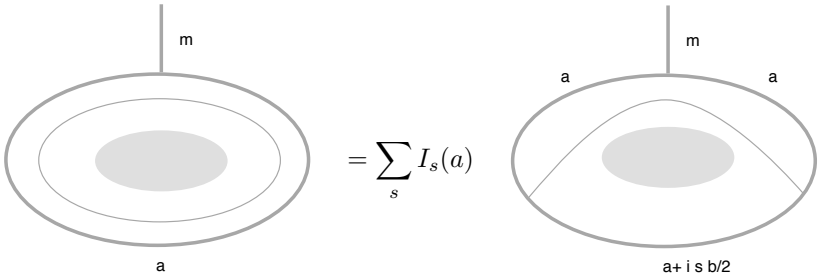


Figure 23. A closed Verlinde line operator wrapping a B-cycle inside the solid torus geometry associated to the one-punctured torus conformal block. The grey ellipse in the picture is a reminder that the loop cannot be shrunk inside the three-dimensional geometry. We depict the first step of the calculation, where an identity line is inserted between the B-cycle loop and the conformal block, and then subject to an A-move

loop of the conformal block, and m the Liouville momentum of the puncture (μ when exponentiated). We depict the cycle, and the first step of the calculation, in figure 23.

Inserting an identity line, and applying an A-move we arrive to a diagram we have already computed, with a degenerate line between two legs of a trinion. The final result is a linear combinations of conformal blocks with parameter $a + isb/2$. We can write the B-cycle operator as

$$\mathcal{L}_{1,0} = \sum_s \imath s p^s \frac{\mu\hat{\alpha}^{-2s}q^{-\frac{1}{2}} + \mu^{-1}\hat{\alpha}^{2s}q^{\frac{1}{2}}}{\hat{\alpha}^2 - \hat{\alpha}^{-2}} = \sum_s \imath s \frac{\mu\hat{\alpha}^{-2s}q^{\frac{1}{2}} + \mu^{-1}\hat{\alpha}^{2s}q^{-\frac{1}{2}}}{\hat{\alpha}^2 - \hat{\alpha}^{-2}} p^s \tag{4.18}$$

If we take the puncture to be the identity, $m = \imath b/2 + \imath b^{-1}/2$, the operator reduces to the expected $p + p^{-1}$.

We can easily compute variants of the B-cycle operator which wind k times around the a edge as they go around the torus, by conjugating the B-cycle operator with a T^k operation on the torus, i.e. the scalar factor $e^{2\pi\imath k\Delta_a}$. Including an extra power of q to untwist the ribbon of the degenerate line we get :

$$\mathcal{L}_{1,k} = (-q^{1/2})^{-k} \sum_s \imath s \hat{\alpha}^{2sk} p^s \frac{\mu\hat{\alpha}^{-2s}q^{-\frac{1}{2}} + \mu^{-1}\hat{\alpha}^{2s}q^{\frac{1}{2}}}{\hat{\alpha}^2 - \hat{\alpha}^{-2}} \tag{4.19}$$

The A- and B- cycle closed Verlinde line operators obey nice algebraic relations which follow from skein relations. For example,

$$\mathcal{L}_{1,0}\mathcal{L}_{0,1} = -q^{-1/2}\mathcal{L}_{1,1} - q^{1/2}\mathcal{L}_{1,-1} \tag{4.20}$$

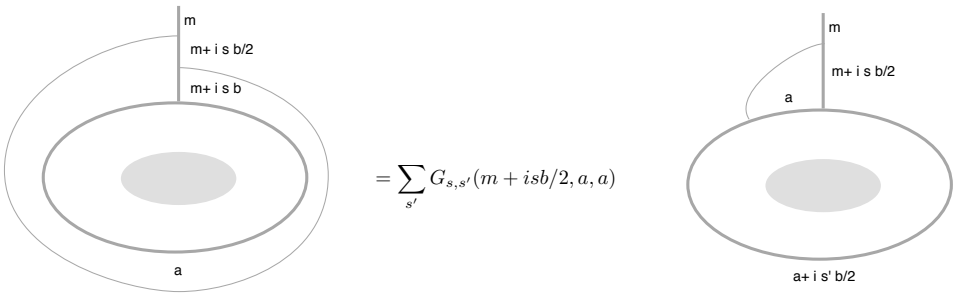


Figure 24. The computation of a "B-cycle" open Verlinde line defect for the one-punctured torus

There are two natural open line operators we will consider on the one-punctured torus. An "A-cycle" open operator looks like the loop in Figure 21 attached to the external leg of the one-punctured torus.

$$\mathcal{O}^s_{0,1} = qp_\mu^{2s} \frac{(\alpha^{1-s}\hat{\mu}q^{s/2} + \alpha^{-1+s}\hat{\mu}^{-1}q^{-s/2})(\alpha^{1-s}\hat{\mu}^{-1}q^{-s/2} + \alpha^{-1+s}\hat{\mu}q^{s/2})}{q - q^{-1}} \tag{4.21}$$

The formula is particularly simple for $s = 1$, where it reduces to

$$-qp_\mu^2 \frac{(\hat{\mu}q^{1/2} + \hat{\mu}^{-1}q^{-1/2})^2}{q - q^{-1}} \tag{4.22}$$

A "B-cycle" open operator involves the calculation in figure 24

5 Applications

5.1 Open Verlinde line operators and quantum Teichmüller theory

The algebraic relations satisfied by open and closed Verlinde line operators, such as the skein relations, can be thought of as a quantum deformation of the algebraic relations satisfied by certain functions on the moduli space of (twisted) $\mathrm{SL}(2, C)$ flat connections over the Riemann surface: traces of holonomies $\mathrm{Tr}\,\mathrm{Hol}_\ell$ and inner products between monodromy eigensections $(\psi_j^{s_j}, \mathrm{Hol}_{\ell_{ij}}\psi_i^{s_i})$ at punctures.

We can make the correspondence very concrete by looking at the semi-classical limit of conformal blocks with extra degenerate insertions. In the semiclassical limit $b \to 0$, keeping finite the classical Liouville momenta $A_i = a_i b$, the BPZ equations satisfied by the "light" degenerate fields $(2, 1)$ in a conformal block reduce to a standard differential equation of the oper form

$$\left[\partial_z^2 + t(z, A_i)\right] \psi(z) = 0 \tag{5.1}$$

where $\psi(z)$ behaves as $dz^{1/2}$ under coordinate transformations, and $t(z, A_i)$ is a classical stress tensor which is such that the solutions have monodromies $-e^{2\pi A_i}$ around the i-th leg of the conformal block. In particular, the solutions behave as $z^{1/2\pm \imath A}$ around a puncture of classical Liouville momentum A. Notice that the peculiar nature of $\psi(z)$, which is a section of the $K^{-1/2}$ bundle on the Riemann surface, means that some care is needed in defining its monodromies, i.e. one has to specify how the local coordinate system is transported.

In general, that is why refer to twisted $\mathrm{SL}(2, C)$ flat connections. This means that one should think of parallel transport along ribbons. A twist of the ribbon can be undone at the price of a factor of -1. This is the semiclassical limit of the usual $-q^{3/2}$.This is why, say, a closed contractible loop with a flat ribbon gives -2 rather than 2.

Thus the semiclassical limit of a conformal block with an extra $(2, 1)$ degenerate puncture at z gives a flat section $\psi(z)$ of the oper. From the explicit form of the $B_s^{\pm}(a)$ matrix, we see that if the degenerate puncture is inserted on a specific edge i and shifts the Liouville momentum by $\imath bs/2$, the corresponding $\psi_{i,s}$ is an eigensection of the monodromy around that edge, with eigenvalues $-\alpha^{-2s}$.

The semiclassical limit of the matrix elements which relate different bases of conformal blocks with the extra degenerate puncture placed on different edges give the matrix elements which relate the corresponding flat eigensections of the oper. Thus, for example, the holonomy of the oper, in a specific basis of eigensections, can be computed from the semiclassical limit of the sequence of A and B moves used to transport the degenerate puncture around the conformal block. Taking some care with following the semiclassical meaning of all intermediate steps in the definitions, it is easy to see that the semiclassical limit of a closed Verlinde line operator is the trace of the holonomy of the oper along the corresponding path on the Riemann surface, while the semiclassical limit of an open line operator between two punctures is the Wronskian of two monodromy eigenvectors at the punctures, transported to a common point along the open path. More generally, the semiclassical limit of a general $|\Gamma\rangle$ evaluates come complicated network of Wilson lines for the oper, possibly ending on monodromy eigensections.

The map from the space of opers in fixed complex structure to the space of twisted $\mathrm{SL}(2, C)$ flat connections over the Riemann surface it not one-to-one: opers give a middle-dimensional, complex Lagrangian submanifold which is encoded in the semiclassical limit of conformal blocks: lhe conformal blocks behave as

$$|a\rangle \sim e^{\frac{1}{b^2}\mathcal{W}[A]} \tag{5.2}$$

and thus the quantum shift operator $\hat{p}^2$ becomes the complexified twist coordinates $p^2 =$

$\exp \partial_A \mathcal{W}[A]$, which combine with the holonomies $\alpha = e^{\pi A}$ to give complexified Fenchel-Nielsen coordinates. Indeed, in the semiclassical limit, the shift operators behave as $\hat{p}^2 = \exp b\partial_a \equiv \exp nb^2\partial_A$. The FN coordinate system is associated to a pair of pants decomposition of the Riemann surface, and the twist coordinate for a leg is defined by comparing two canonical normalizations for the monodromy eigensections for a leg of the pair of pants decomposition. The two canonical normalizations are associated to either of the trinions joined by the leg, and use the data of the monodromy eigensections at the other legs of each trinion. This matches well with the semiclassical limit of the degenerate field holonomy: the specific form of the A move coefficients fix the relative normalization of all the eigensections for a trinion, and the comparison between nearby trinions involve the transport of the degenerate field along the leg, which shifts the Liouville momentum by $\pm b/2$ and rescales the flat sections by $p^{\pm 1}$.

At least locally, if we allow the complex structure parameters to vary as well, we can parameterize the full space of flat connections. Furthermore, before we act with the Verlinde line operators on the conformal blocks, they are given as a function of the A-cycle holonomies A_i of the oper and their conjugate momenta $\log p_i$. The sequence of elementary moves we use to compute them provides a quantization of rules which work for any twisted $\mathrm{SL}(2, C)$ flat connection, not just for an oper.

Thus we claim that the semiclassical limits of the operators O_ℓ and $O_{\ell_{12}}$ evaluate respectively the trace of the holonomy along a curve ℓ or the antisymmetric inner product of two monodromy eigensections compared along a path ℓ_{12} for a twisted flat connection labelled by the FN coordinates A_i and $\log p_i$. When acting on conformal blocks, that specializes to the holonomy and Wronskians for the corresponding oper.

The inner products $(\psi_j^{s_j}, \mathrm{Hol}_{\ell_{ij}} \psi_i^{s_i})$ of two monodromy eigensections at punctures, specialized to the ℓ_{ij} being edges of an ideal triangulation and to a fixed choice of s_i, are the building blocks for Fock/shear coordinates on Teichmüller space. More precisely, Fock coordinates are cross-ratios which do not depend on the choice of normalization of the eigensections. Thus we expect the open Verlinde line operators to be useful in understanding the relation between the quantization of Teichmüller space in FN coordinates and in Fock coordinates.

Conventionally, the standard presentation of the quantization of Teichmüller space starts with Fock coordinates and uses them to reconstruct systematically the quantization of the traces of holonomies [7]. Conformal blocks and quantum Teichmüller theory are related to each other through a Riemann-Hilbert problem [13, 14]. Our alternative approach based on open Verlinde line operators proceeds in the opposite direction, from conformal blocks and FN coordinates to quantum Teichmüller theory.

It is easy to match our proposal for the quantum Wronskians and their cross-ratios with the explicit expressions computed for the one-punctured torus in [15]. It should

be possible to also compare our results with the general integral kernels constructed in [16], which intertwine FN and Fock coordinates for the same Riemann surface.

5.2 Relation to q-deformed traffic rules and refined framed BPS degeneracies

It is natural to conjecture, based on general supersymmetric gauge theory considerations, that the relation between Verlinde line operators and quantum Fock coordinates encodes the refinement of framed BPS degeneracies for theories in the class A_1, as defined and studied in [8].

The framed BPS degeneracies should be encoded in the expansion of general Verlinde line operators in terms of the collection of open Verlinde line operators

$$\hat{O}_{ij} \equiv \hat{O}_{\ell_{ij}}^{s_i,s_j} \tag{5.3}$$

associated to a choice of ideal triangulation with edges ℓ_{ij} and a fixed choice of shifts s_i, which picks a specific quantum eigensection. These are the quantum version of the objects denoted as "(s_i, s_j)" in that reference, where "s_i" denoted a choice of eigensection at each vertex.

In the cluster algebra language, the Fock coordinates/cross-ratios used in [8] are X-type variables, while the O_{ij} operators are A-type coordinates. It is useful to cast our results in terms of the O_{ij} rather than their cross-ratios. In particular, rather than expressing some operator $\hat{O}_\ell$ as a Laurent polynomial in the cross-ratios, we will write something like

$$\hat{O}_\ell \prod_{(i,j)|\ell_{ij}\cap\ell\neq 0} \hat{O}_{ij}^{\#(\ell_{ij}\cap\ell)} = \sum_{n_{ij}} c_{n_{ij}}[q] \prod_{i,j} \left(\hat{O}_{ij}\right)^{n_{ij}} \tag{5.4}$$

Here ℓ can be a closed path, or any open path with s_i labels at the ends. The n_{ij} are non-negative powers, such that $\sum_j n_{ij}$ equals the number of times operators of the type $\hat{O}_{i,\cdot}$ appear on the left hand side. The $c_{n_{ij}}[q]$ are Laurent polynomials in q.

To get such an expression, we multiply $\hat{O}$ by an appropriate power of the operators associated to each of the edges ℓ_{ij} crossed by ℓ. That will allow us to use the skein relations to break ℓ into pieces, until each term of the sum only involves only a collection of paths associated to the edges of the triangulation. This can be done recursively, eliminating the intersections one-by-one and breaking ℓ into smaller pieces.

The semi-classical limit of the skein operation applied to a product $\hat{O}_\ell \hat{O}_{ij}$ is very simple: it corresponds to inserting in the holonomy along ℓ a complete basis

$$1 = \frac{(\cdot,\psi_i)(\psi_j,\cdot) - (\cdot,\psi_j)(\psi_i,\cdot)}{(\psi_i,\psi_j)} \tag{5.5}$$

which is the basic step of the traffic rules discussed in [8].

5.3 Quantum groups

There is a deep relation between conformal blocks and quantum groups. The most striking example is the fact that the fusion kernel for Virasoro conformal blocks coincides with the fusion kernel for the modular double quantum enveloping algebra $\mathcal{U}_q(sl(2,R)) \times \mathcal{U}_{\tilde{q}}(sl(2,R))$, with $q = e^{i\pi b^2}$ and $\tilde{q} = e^{i\pi b^{-2}}$. This relation and others involving Clebsh-Gordan coefficients is discussed in detail in [9], which establishes a dictionary between the quantum groups and certain structures in quantum Teichmüller theory.

In this section we would like to complement that analysis by attempting to reconstruct directly an action of the modular double quantum enveloping algebra onto a certain space of conformal blocks. The quantum group generators in $\mathcal{U}_q(sl(2,R))$ will take the form of certain open Verlinde line operators labelled by the $(3,1)$ degenerate momentum, and the dual generators in $\mathcal{U}_q(sl(2,R))$ will take the form of certain open Verlinde line operators labelled by the $(1,3)$ degenerate momentum.

Our construction will be simply a re-formulation of a beautiful construction given in [10] in the context of Chern-Simons theory. In that reference, quantum group generators are built as operators which add rungs to webs of Wilson lines in Chern-Simons theory. The 3d TFT combinatorics of the construction is exactly the same as for open Verlinde line operators acting on conformal blocks, and even the fusion and braiding coefficients will be closely related, as the ones for conformal blocks, at least if all momenta are specialized to degenerate values, are closely related to those for Wilson loops in Chern-Simons theory.

A crucial step in the construction in [10] actually works somewhat more naturally for conformal blocks: in order to recover the quantum group generators, the spin label of a certain reference line has to be analytically continued to infinity. For conformal blocks, no analytic continuation is needed, as the momenta lie naturally in the continuum range. Furthermore, the limit as the momentum of an external leg is sent to infinity can be done in such a way that the standard space of conformal blocks is mapped to another well-defined space of conformal blocks: conformal blocks with an irregular singularity [17].

More precisely, if we start from a regular conformal block, pick two external legs with momenta a_2 and $a_0 - a_2$ and send a_2 to infinity while scaling the distance z between the punctures to zero while keeping $\Lambda = a_2 z$ fixed, we obtain a conformal block with an irregular singularity of rank 1. The parameter Λ behaves as a generalized complex structure parameter, while a_0 behaves much as a Liouville momentum.

The BPZ equation has irregular singularities, and Stokes phenomena. One can still discuss the transport of degenerate fields around the Riemann surface, and define canon-

ical bases of solutions of the BPZ equations with prescribed asymptotic behaviour at the irregular singularity, which behaves in a similar fashion as the bases of monodromy eigenstates around regular punctures. Thus there are well-defined generalizations to the irregular case of standard conformal block notions, fusion and braiding operations, etc. Both closed and open Verlinde line operators should remain meaningful in the limit. Even operators which end on a leg whose momentum is sent to infinity, such as $O_k^{s_1,s_2}$, will have a meaningful limit.

We leave the development of the full 3d TFT-like machinery for irregular conformal blocks to a separate publication. Here we will just focus on the algebraic aspects of the $a_2 \to \infty$ limit which are useful to make contact with the theory of quantum groups.

We can look more closely at the algebra generated by open line defects stretched between two fixed edges. We can consider defects $O_k^{s_1,s_2}$ in the $(k+1,1)$ representation, which shift the Liouville momenta of the edges by $\imath s_1 b/2$ and $\imath s_2 b/2$. These operators form a closed algebra under multiplication. Indeed, we can fuse the line defects with an A-move, and then eliminate the triangles.

We already computed the structure constants involving O_1 and any O_k:

$$\begin{aligned}
\hat{O}_1^{s_1,s_2}\hat{O}_k^{s_1',s_2'} &= \sum_{s=\pm 1} C^{k;s}_{-s_1,-s_2;-s_1',-s_2'}[\hat{a}_1,\hat{a}_2]\hat{O}_{k+s}^{s_1+s_1',s_2+s_2'} \\
\hat{O}_k^{s_1',s_2'}\hat{O}_1^{s_1,s_2} &= \sum_{s=\pm 1} \hat{O}_{k+s}^{s_1+s_1',s_2+s_2'} C^{k;s}_{s_2,s_1;s_2',s_1'}[\hat{a}_2,\hat{a}_1]
\end{aligned} \tag{5.6}$$

In the above sums we should set to zero terms where $s_1 + s_1'$ or $s_2 + s_2'$ lie outside the allowed range of shifts for the $\hat{O}_{k-1}$ operator. Notice the relative order of coefficients and operators, which matter because $\hat{\alpha}_1 O_t^{s_1,s_2} = q^{s_1/2} O_t^{s_1,s_2}\hat{\alpha}_1$, etc.

Remember the explicit expression

$$\begin{aligned}
C^{k;s}_{s_2,s_3;s_2',s_3'}[a_2,a_3] = s s_2 s_3 &\frac{\alpha_2^{1-s} q^{s_2(k+2)/2+s_2'/2} - \alpha_2^{s-1} q^{-s_2(k+2)/2-s_2'/2}}{q^{k+1}-q^{-k-1}} \cdot \\
&\cdot \frac{\alpha_3^{1-s} q^{s_3(k+2)/2+s_3'/2} - \alpha_3^{s-1} q^{-s_3(k+2)/2-s_3'/2}}{q-q^{-1}}
\end{aligned} \tag{5.7}$$

The two expressions match for $k = 1$:

$$\begin{aligned}
O_1^{s_1,s_2}O_1^{s_1',s_2'} =& (q+q^{-1})^{\delta_{s_1,s_1'}+\delta_{s_2,s_2'}-1} O_2^{s_1+s_1',s_2+s_2'} + \\
&- \frac{\delta_{s_1+s_1',0}\delta_{s_2+s_2',0}}{q+q^{-1}} \frac{\hat{\alpha}_1^{2s_1} q - \hat{\alpha}_1^{-2s_1} q^{-1}}{q-q^{-1}} \frac{\hat{\alpha}_2^{2s_2} q - \hat{\alpha}_2^{-2s_2} q^{-1}}{q-q^{-1}}
\end{aligned} \tag{5.8}$$

In order to get a more standard algebraic structure, one could limit the s_i shifts to be zero (and thus only use $(2k+1,1)$ defects). The problem is that the result is

somewhat boring. The operators $O_{2k}^{0,0}$ can be written recursively as degree k polynomials in $O_2^{0,0}$ and the algebra reduces to the algebra of polynomials in one variable.

The next simplest case is to focus on operators with $s_1 = 0$. They commute with $\hat{\alpha}_1$. We can write a neat set of relations concerning the subset O_2^{0,s_2}. We can define $J^+ = (q - q^{-1})O_2^{0,2}$ and $J^- = (q - q^{-1})O_2^{0,-2}$. Then we define

$$\begin{aligned} J^0 &\equiv (\hat{\alpha}_2^2 - \hat{\alpha}_2^{-2})^{-1}(J^+J^- - J^-J^+) = \\ &= (\alpha_1^2 + \alpha_1^{-2})\frac{q - q^{-1}}{q + q^{-1}}O_2^{0,0} + \frac{(\alpha_1^2 q - \alpha_1^{-2}q^{-1})(\alpha_1^2 q^{-1} - \alpha_1^{-2}q)}{q^2 - q^{-2}}(\hat{\alpha}_2^2 + \hat{\alpha}_2^{-2}) \end{aligned} \tag{5.9}$$

We get interesting algebraic relations

$$\begin{aligned} J^0J^- - J^-J^0 &= (q + q^{-1})(\hat{\alpha}_2^2 q - \hat{\alpha}_2^{-2}q^{-1})J^- \\ J^0J^+ - J^+J^0 &= (q + q^{-1})(\hat{\alpha}_2^2 q^{-1} - \hat{\alpha}_2^{-2}q)J^+ \end{aligned} \tag{5.10}$$

We should also record the relation

$$\begin{aligned} &(\hat{\alpha}_2^2 q - \hat{\alpha}_2^{-2}q^{-1})O_2^{0,2}O_2^{0,-2} + (\hat{\alpha}_2^2 q^{-1} - \hat{\alpha}_2^{-2}q)O_2^{0,-2}O_2^{0,2} - \frac{(\hat{\alpha}_2^2 - \hat{\alpha}_2^{-2})}{q + q^{-1}}O_2^{0,0}O_2^{0,0} = \\ &= -(\hat{\alpha}_2^2 q - \hat{\alpha}_2^{-2}q^{-1})(\hat{\alpha}_2^2 q^{-1} - \hat{\alpha}_2^{-2}q)(\hat{\alpha}_2^2 - \hat{\alpha}_2^{-2})\frac{(\alpha_1^2 q - \alpha_1^{-2}q^{-1})(\alpha_1^2 q^{-1} - \alpha_1^{-2}q)}{(q + q^{-1})(q - q^{-1})^4} \end{aligned} \tag{5.11}$$

We are ready to make contact with [10]: in order to simplify the algebra, we send a_2 to infinity.

Our explicit examples and consistency of the composition of operators suggest setting $O_k = \hat{\alpha}_2^k o_k$ and keeping the o_k finite in the limit. We thus define $J^a = \hat{\alpha}_2^2 t^a$ and the relations

$$\begin{aligned} t^0 \equiv q^{-2}t^+t^- - q^2 t^-t^+ &= (\alpha_1^2 + \alpha_1^{-2})\frac{q - q^{-1}}{q + q^{-1}}o_2^{0,0} + \\ &+ \frac{(\alpha_1^2 q - \alpha_1^{-2}q^{-1})(\alpha_1^2 q^{-1} - \alpha_1^{-2}q)}{q^2 - q^{-2}} \end{aligned} \tag{5.12}$$

and

$$\begin{aligned} q^{-1}t^0t^- - qt^-t^0 &= (q + q^{-1})t^- \\ qt^0t^+ - q^{-1}t^+t^0 &= (q + q^{-1})t^+ \end{aligned} \tag{5.13}$$

and the Casimir-like expression

$$q^{-1}o_2^{0,2}o_2^{0,-2} + qo_2^{0,-2}o_2^{0,2} - \frac{1}{q+q^{-1}}o_2^{0,0}o_2^{0,0} = \\ = -\frac{(\alpha_1^2 q - \alpha_1^{-2}q^{-1})(\alpha_1^2 q^{-1} - \alpha_1^{-2}q)}{(q+q^{-1})(q-q^{-1})^4} \tag{5.14}$$

These are the quantum group relations found in [10].

We can present some examples of quantum group representations which emerge from simple graphs Γ_0. This will also help in making contact with [9]. First, we can take Γ_0 to be the trinion. In this special case we will have to also sent α_3 to infinity in order to have a good irregular conformal block limit, keeping $\alpha_2\alpha_3 = \alpha_0$ fixed. The result will be that our operators will act on irregular conformal blocks with one regular puncture and one irregular puncture.

We have

$$O_1^{s_1,s_2} = -1\frac{\hat{\alpha}_3\hat{\alpha}_2^{-s_1}\hat{\alpha}_1^{-s_2}q^{\frac{s_1 s_2}{2}} + \hat{\alpha}_3^{-1}\hat{\alpha}_2^{s_1}\hat{\alpha}_1^{s_2}q^{\frac{-s_1 s_2}{2}}}{q-q^{-1}}\hat{p}_1^{s_1}\hat{p}_2^{s_2} \tag{5.15}$$

We get

$$J^+ = -\frac{(\hat{\alpha}_1\hat{\alpha}_3^{-1}\hat{\alpha}_2^{-1}q^{1/2} + \hat{\alpha}_1^{-1}\hat{\alpha}_3\hat{\alpha}_2 q^{-1/2})(\hat{\alpha}_1\hat{\alpha}_3^{-1}\hat{\alpha}_2 q^{-1/2} + \hat{\alpha}_1^{-1}\hat{\alpha}_3\hat{\alpha}_2^{-1}q^{1/2})}{q-q^{-1}}p_2^{-2} \\ J^- = -\frac{(\hat{\alpha}_1\hat{\alpha}_3\hat{\alpha}_2 q^{1/2} + \hat{\alpha}_1^{-1}\hat{\alpha}_3^{-1}\hat{\alpha}_2^{-1}q^{-1/2})(\hat{\alpha}_1\hat{\alpha}_3\hat{\alpha}_2^{-1}q^{-1/2} + \hat{\alpha}_1^{-1}\hat{\alpha}_3^{-1}\hat{\alpha}_2 q^{1/2})}{q-q^{-1}}p_2^2 \tag{5.16}$$

Then we compute

$$J^0 = -\frac{(\hat{\alpha}_1^2 + \hat{\alpha}_1^{-2})(\hat{\alpha}_3^2 + \hat{\alpha}_3^{-2}) + (\hat{\alpha}_2^2 + \hat{\alpha}_2^{-2})(q+q^{-1})}{q-q^{-1}} \tag{5.17}$$

which satisfies the desired commutation relations.

Next, we take the limit $\alpha_2 \to \infty$ at fixed $\alpha_0 = \alpha_2\alpha_3$:

$$t^+ = -\frac{\alpha_1^2\hat{\alpha}_0^{-2} + q^{-1}}{q-q^{-1}}p_0^{-2} \\ t^- = -\frac{q + \alpha_1^{-2}\hat{\alpha}_0^{-2}}{q-q^{-1}}p_0^2 \\ t^0 = -\frac{(\alpha_1^2 + \hat{\alpha}_1^{-2})\hat{\alpha}_0^{-2} + q + q^{-1}}{q-q^{-1}} \tag{5.18}$$

We can make contact with a more familiar form of the quantum group algebra if we define

$$\begin{aligned} K &= \hat{\alpha}_0 \\ E &= \hat{\alpha}_0 t^+ \\ F &= \hat{\alpha}_0 t^- \end{aligned} \tag{5.19}$$

Indeed,

$$[E, F] = \hat{\alpha}_0^2 q^{-1} t^+ t^- - \hat{\alpha}_0^2 q t^- t^+ = -\frac{\hat{\alpha}_0^2 - \hat{\alpha}_0^{-2}}{q - q^{-1}} \tag{5.20}$$

This is basically the same as the basic quantum group representation discussed in [9].

If we repeat the exercise for more interesting graphs Γ_0, we will obtain several distinct simultaneous actions of quantum group generators on the space of conformal blocks with an irregular puncture and n regular punctures. Each action will be labelled by one of the regular punctures, and a path from the irregular puncture to the regular punctures.

Different sets of quantum group generators associated to paths which only intersect at the irregular puncture will have some twisted commutation relations governed by the $\alpha_2 \to \infty$ of the braiding matrix for two $(3, 1)$ insertions on an edge of momentum a_2.

Different bases of irregular conformal blocks will give different representations of the quantum group generators, intertwined by the fusion and braiding kernels for conformal blocks. With some extra work, it should be possible to identify some of these representations with the twisted tensor product representations employed in [9], and thus show the match between conformal block and quantum group fusion kernels and R-matrices.

It would also be interesting to explore the representations associated to punctures on a higher genus Riemann surface.

Acknowledgements

DG thanks Joerg Teschner for discussions and comments on the draft. Much of this work was developed as a result of useful questions, discussions and suggestions by Jaume Gomis, Bruno Le Floch and Edward Witten. We also thank Alexander Braverman for rekindling DG interest in this subject. The research of DG was supported by the Perimeter Institute for Theoretical Physics. Research at Perimeter Institute is supported by the Government of Canada through Industry Canada and by the Province of Ontario through the Ministry of Economic Development and Innovation.

References

[1] E. P. Verlinde, *Fusion Rules and Modular Transformations in 2D Conformal Field Theory*, *Nucl.Phys.* **B300** (1988) 360.

[2] N. Drukker, J. Gomis, T. Okuda, and J. Teschner, *Gauge Theory Loop Operators and Liouville Theory*, *JHEP* **1002** (2010) 057, [arXiv:0909.1105].

[3] L. F. Alday, D. Gaiotto, S. Gukov, Y. Tachikawa, and H. Verlinde, *Loop and surface operators in N=2 gauge theory and Liouville modular geometry*, *JHEP* **1001** (2010) 113, [arXiv:0909.0945].

[4] J. Gomis, T. Okuda, and V. Pestun, *Exact Results for 't Hooft Loops in Gauge Theories on S4*, *JHEP* **1205** (2012) 141, [arXiv:1105.2568].

[5] N. Drukker, D. Gaiotto, and J. Gomis, *The Virtue of Defects in 4D Gauge Theories and 2D CFTs*, *JHEP* **1106** (2011) 025, [arXiv:1003.1112].

[6] J. Fjelstad, J. Fuchs, and C. Stigner, *RCFT with defects: Factorization and fundamental world sheets*, *Nucl.Phys.* **B863** (2012) 213–259, [arXiv:1202.3929].

[7] J. Teschner, *An analog of a modular functor from quantized Teichm"uller theory*, *ArXiv Mathematics e-prints* (Oct., 2005) [math/0510174].

[8] D. Gaiotto, G. W. Moore, and A. Neitzke, *Framed BPS States*, arXiv:1006.0146.

[9] I. Nidaiev and J. Teschner, *On the relation between the modular double of U_q(sl(2,R)) and the quantum Teichmueller theory*, *ArXiv e-prints* (Feb., 2013) [arXiv:1302.3454].

[10] E. Witten, *Gauge Theories, Vertex Models and Quantum Groups*, *Nucl.Phys.* **B330** (1990) 285.

[11] E. Witten, *Fivebranes and Knots*, arXiv:1101.3216.

[12] D. Gaiotto and E. Witten, *Knot Invariants from Four-Dimensional Gauge Theory*, *Adv.Theor.Math.Phys.* **16** (2012), no. 3 935–1086, [arXiv:1106.4789].

[13] J. Teschner, *From Liouville theory to the quantum geometry of Riemann surfaces*, hep-th/0308031.

[14] G. Vartanov and J. Teschner, *Supersymmetric gauge theories, quantization of moduli spaces of flat connections, and conformal field theory*, arXiv:1302.3778.

[15] T. Dimofte and S. Gukov, *Chern-Simons Theory and S-duality*, *JHEP* **1305** (2013) 109, [arXiv:1106.4550].

[16] T. Dimofte, D. Gaiotto, and R. van der Veen, *RG Domain Walls and Hybrid Triangulations*, arXiv:1304.6721.

[17] D. Gaiotto and J. Teschner, *Irregular singularities in Liouville theory and Argyres-Douglas type gauge theories, I*, *JHEP* **1212** (2012) 050, [arXiv:1203.1052].